https://doi.org/10.1016/j.seppur.2019.115817

Energy-efficient extractive pressure-swing distillation for separating binary minimum azeotropic mixture dimethyl carbonate and ethanol

Ao Yang[a,b], Shirui Sun[a,b], Tao Shi[a,b], Di Xu[c], Jingzheng Ren[d], and Weifeng Shen [a,b,*]

[a]School of Chemistry and Chemical Engineering, Chongqing University, Chongqing 400044, China

[b]National-municipal Joint Engineering laboratory for Chemical Process Intensification and Reaction, Chongqing University, Chongqing 400044, China

[c]College of Chemistry and Chemical Engineering, Chongqing University of Science & Technology, Chongqing, 401331, China

[d]Department of Industrial and Systems Engineering, The Hong Kong Polytechnic University, Hong Kong SAR, China

Corresponding Author: *(W. Shen) E-mail: shenweifeng@cqu.edu.cn

Abstract: An energy-efficient extractive pressure-swing distillation process is proposed for separating binary minimum azeotropic mixture ethanol and dimethyl carbonate. It can be observed that the minimum amount flow rate of entrainer will be decreased when the operating pressure of extractive distillation column is increased via the thermodynamic feasibility insights (i.e., residue curve map and isovolatility lines). Therefore, an extractive pressure-swing distillation process with 4 bar for the extractive distillation column is designed. Process variables of the proposed design are optimized by combining the sensitivity analysis and sequence quadratic program approaches with minimum total annual cost as objective function. Total annual cost, CO_2 emissions, and exergy loss of the optimized extractive pressure-swing distillation with 4 bar for the extractive distillation column is reduced by 44.09%, 44.16% and 41.54%,

respectively when compared with the existing process with 1 bar for the extractive distillation column, which mainly attributing the flow rate of entrainer decreasing from 200.020 kmol/h to 44.963 kmol/h. Furthermore, the extractive pressure-swing distillation with heat integration is studied to further reduce energy cost because the enough heat transfer temperature difference could be provided by increasing operation pressure.

Keywords: Extractive pressure-swing distillation; azeotropic mixture; separation; energy-efficient; conceptual design

Notation

ED extractive distillation

EPSD extractive pressure-swing distillation

TAC total annual cost [10^6 US$]

TOC total operating cost [10^6 US$]

TCC total capital cost [10^6 US$]

EtOH ethanol

DMC dimethyl carbonate

PX *p*-xylene

EDC extractive distillation column

ERC entrainer recovery column

HP high pressure

MP medium pressure

LP low pressure

SQP sequence quadratic program

CPOM complete process optimization model

N_{FE} feed location of entrainer

N_{F1} feed location of fresh feed

N_{F2} feed location of ERC

F_E flowrate of entrainer [kmol/h]

D distillate rate [kmol/h]

1. Introduction

Extractive distillation [1-7], pressure-swing distillation [8-12], azeotropic distillation [13-18] are frequently applied in petroleum, chemical and pharmaceutical industries to separate azeotropic or close-boiling mixtures. According to the survey, about 45-55% of energy is consumed in the separation process [19]. In addition, energy consumption of the extractive distillation (ED) process accounts for 10-15% in the separation section [19]. Based on the listed descriptions, much attention has been attracted to develop an energy-saving ED process (e.g., developing intensified configurations, screening suitable entrainers and changing operating pressures) because it has great significance to sustainable developments.

Many researchers are committed to develop novel separation configurations to achieve energy-saving and CO_2 emission-reduction. For instance, Kiss and Suszwalak [20] proposed an intensified extractive and azeotropic dividing wall columns for ethanol dehydration and they demonstrated that the energy consumption could be reduced by 10–20%. Following that, a novel decanter assisted extractive dividing wall column for separating heterogeneous system methanol/toluene/water with multi-azeotrope are proposed in our previous work [21]. Tututi-Avila et al [22]. proposed an energy-saving side-stream ED process for separating

azeotropic (i.e., ethanol/water and acetone-methanol) and close-boiling mixtures (i.e., heptane-toluene) and they proved that the total annual cost (TAC), energy consumption and CO_2 emissions are significantly decreased through the proposed side-stream scheme. Sun et al. reported an intensified extractive dividing wall column to separate binary azeotropic mixtures benzene/cyclohexane [23] and they proved that the steam consumption could be significantly decreased. Several alterative separation configurations (e.g., side-stream and thermally coupled ED) are then investigated to separate ternary mixture acetonitrile/benzene/methanol with multi-azeotrope as explored by Wang et al. [24] and they illustrated that the side-stream configuration has the best performances in economics and environmental protection.

In addition, selecting suitable entrainer is very important to increase the relative volatility in achieving the energy-saving and emissions reduction. For example, triethylene glycol is chosen as the suitable entrainer for separating 1,2-propanediol and ethylene glycol because the relative volatility is largely improved [25]. A best entrainer is screened out to find the ED with minimum total annual cost for azeotropes mixtures methanol/acetone separation [26]. Following that, three alternative entrainers (i.e., n-methyl-2-pyrrolidone, dimethyl sulfoxide and ethylene glycol) are used to mixture acetone/chloroform with a maximum-boiling azeotrope and the results shown that the TAC and the amount of entrainer could be significantly reduced with n-methyl-2-pyrrolidone as the entrainer [27]. The triple-column extractive distillation processes with single and mixed entrainer are explored to separate ternary azeotropic mixture tetrahydrofuran/ethanol/water [28]. The comparison of infinite dilution activity coefficient ratio and uni-volitility lines were explored to screen best entrainer for separating ternary mixtures isopropyl alcohol/isopropyl acetate/water [29]. Pan et al. investigated an energy-saving extractive

distillation for ethanol dehydration using deep eutectic entrainer [30]. Recently, Yang et al. [31] proposed an energy-saving triple-column extractive distillation scheme via the reduction of pressure and screening of suitable entrainer for separating ethyl acetate/ethanol/water system and the TAC of the proposed scheme is demonstrated could be reduced by 14.11%.

To reduce energy consumption and CO_2 emissions, change operating pressure (i.e., change of relative volatility) is another effective way [32]. Li et al. [33] reported several energy-saving ED schemes (e.g., ED with low operating pressure and extractive dividing wall column) for the separation of binary mixtures 2-methoxyethanol/toluene. You et al. [34] explored an energy-saving ED scheme for the separation of diisopropylether/isopropyl alcohol via the operation at low pressure and the results demonstrated that the mount of entrainer could be reduced by enhancing the relative volatility at 0.4 atm. An energy-efficient ED by varying pressure is proposed and they displayed that the amount of entrainer could be decreased from 1900 kmo/h at 1 atm to 858.4 kmol/h at 10 atm resulting in a sharp decrease in energy consumption [35]. ED schemes with and without heat integration to separate tetrahydrofuran/water mixture by changing the operating pressure are explored by Gu et al. [36] and they then investigated an energy-efficient heat integrated assisted ED design at low pressures for separating the ternary mixture tetrahydrofuran/methanol/water with two azeotropes [37]. Besides, effects of operating pressure on univolatility lines (i.e., the amount of entrainer) have also been reported by Wang et al. [38].

To the best of our knowledge, few studies have been reported the extractive distillation scheme for the separation of minimum-boiling azeotropic system ethanol/dimethyl carbonate (EtOH/DMC) through varying pressure to achieve energy-saving. Hence, we propose a

systematic procedure for optimal design an extractive pressure-swing distillation (EPSD) to separate minimum azeotropic mixtures. Effects of pressure on total annual cost and minimum flow rate of entrainer are firstly studied via thermodynamic feasibility insights (e.g., univolatility lines and residue curve maps). Design parameters of the proposed EPSD scheme (e.g., feed locations, reflux ratio and flow rate of entrainer) are then optimized by combining the sensitivity analysis and sequence quadratic program (SQP) approaches. Following that, the heat integration EPSD process is proposed to further save energy through changing operating pressures of entrainer recovery columns. Finally, three indicators CO_2 emissions, total annual cost and exergy loss are introduced to compare the environmental, economic, and thermodynamic efficiency of the proposed EPSD with and without heat integration.

2. Existing Extractive Distillation Process

DMC and EtOH as important solvents [39] are frequently generated in synthesis of diethyl carbonate or methyl ethyl carbonate [40, 41], which are required to be separated to avoid causing environmental issues. However, the mixture of DMC/EtOH could not be separated via the conventional distillation because it could form minimum azeotrope at atmosphere pressure. According to the report of Gao's group [41], *p*-xylene (PX) is determined as the best entrainer among PX, butyl propionate and isobutyl acetate to separate EtOH/DMC via the extractive distillation.

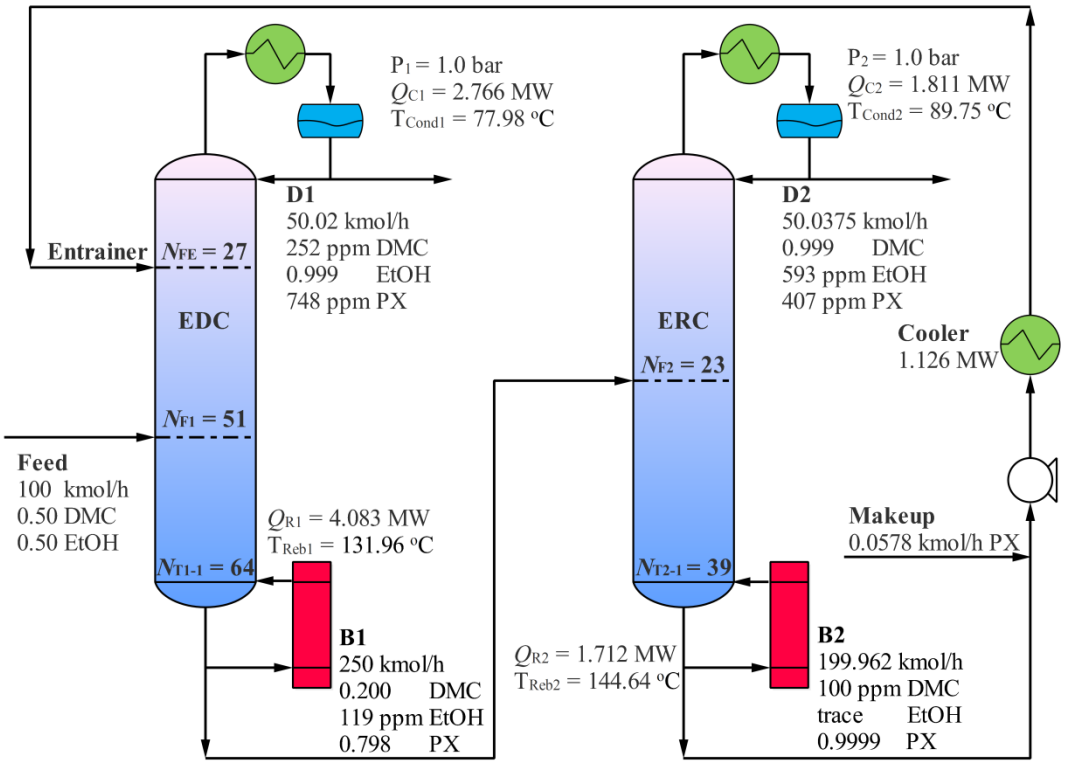

Figure 1. Existing extractive distillation process for separating EtOH/DMC mixture

In the study of Liu et al. [41], existing conventional extractive distillation scheme (denoted as design 1) with detailed information for separating EtOH/DMC azeotropic mixture is illustrated in Figure 1. Extractive distillation column (EDC) with 65 theoretical trays and entrainer recovery column (ERC) with 40 theoretical trays are both operated at 1.0 bar. Entrainer and fresh feed are fed to 27th and 51th stages of the EDC, respectively. The azeotrope of DMC/EtOH could be broken in the extractive distillation section (from 27th to 51th stages in EDC) and then the EtOH is distilled as the overhead product. DMC and PX from the bottom of EDC are fed to 23th stages of the ERC. DMC is obtained as the distillate product while the high purity entrainer is obtained in the bottom stream and then is recycled to the EDC with a small quantity of PX.

3. Methodology

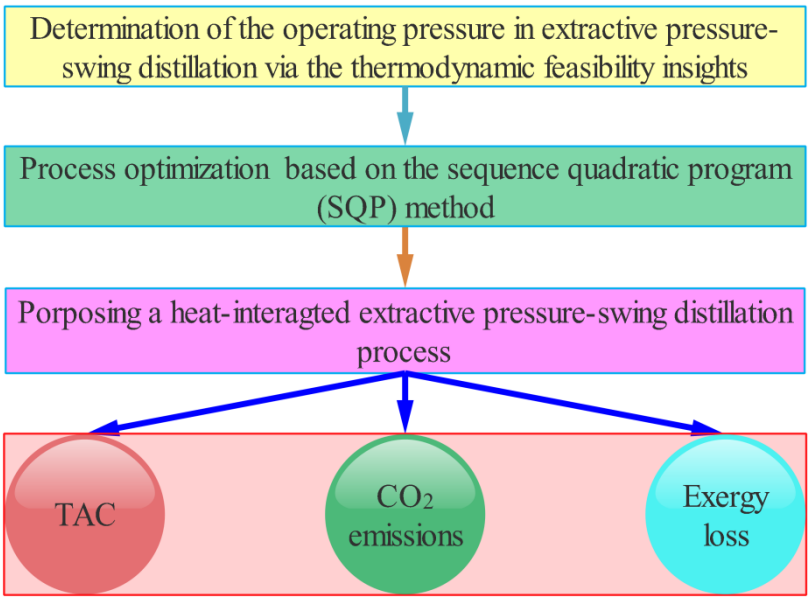

Figure 2. Proposed systematic approach for energy-efficient extractive pressure-swing distillation to separate EtOH/DMC azeotropic mixture

Herein, a systematic approach for energy-efficient EPSD scheme to separate EtOH/DMC azeotropic mixture is proposed in Figure 2. Effect of operating pressure of the EDC on minimum entrainer flow rate is firstly investigated based on thermodynamic feasibility insights (e.g., univolatility lines and residue curve maps). After that, optimization of the proposed design is performed by combining the SQP and sensitivity analysis to obtain the optimal parameters (e.g., feed locations and reflux ratio) with minimum TAC. Subsequently, a heat-integrated EPSD process is proposed to further reduce the energy consumption by varying the operating pressure of ERC. Finally, TAC, CO_2 emissions and exergy loss are introduced to evaluate the impacts of proposed approach on economy, environment and thermodynamics efficiency.

3.1 Thermodynamic analysis

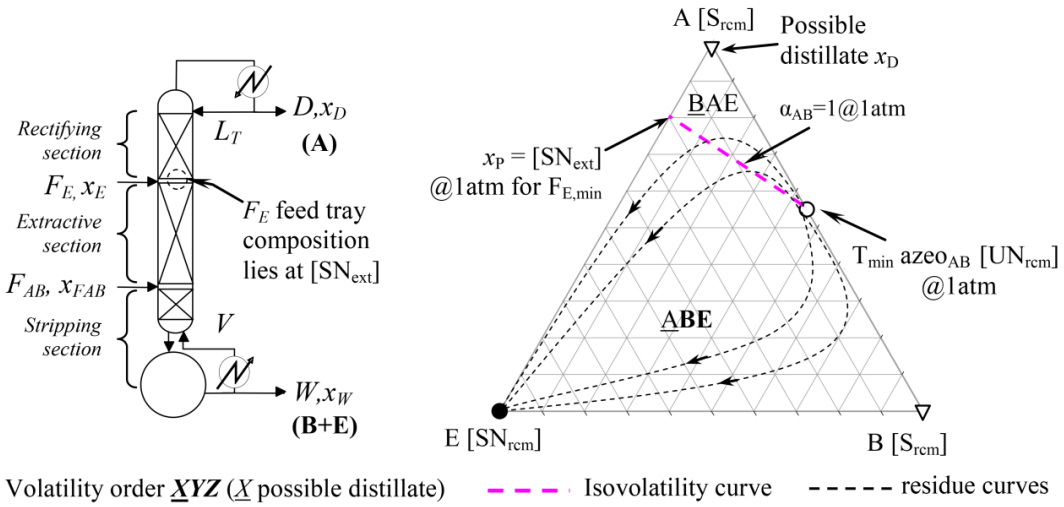

Figure 3. Extractive distillation scheme and thermodynamic features of class 1.0-1a at 1 atm

Figure 3 illustrates the extractive distillation scheme and thermodynamic features of class 1.0-1a at 1 atm. In the extractive distillation process, the ternary diagram is divided into two regions (BAE and ABE) via the isovolatility curve $\alpha_{AB} = 1$. The intersection of isovolatility curve $\alpha_{AB} = 1$ and the binary side A-E while the intersection point is denoted as x_P. Of note is that, the closer between the intersection to key component (i.e., small value of x_P), the less the amount of entrainer is employed indicating lower energy and capital costs [26, 42, 43].

3.2 Optimization

In this work, the proposed process is optimized based on the SQP solver, which is reported by our previous study [10]. Optimization approach involving objective function, constraints, and variable bounds is carried out in the Aspen Plus.

3.2.1 Objective function

TAC is introduced as the objective function in optimizing the proposed EPSD scheme. According to our previous work [10], TAC is sensitive to the key operational variables reflux ratio, feed locations and entrainer flow rates (see Eq. (1)).

$$\min \ \mathrm{TAC} = f(N_{F1}, N_{FE}, N_{F2}, RR_1, RR_2, F_E, D_1, D_2) \tag{1}$$

where N_{F1} and N_{FE} represent feed locations of azeotropic mixture and entrainer, respectively; N_{F2} refers to feed location of ERC; RR_1 and RR_2 are the reflux ratio of two columns; D_1, and D_2 represent the distillate rates; flow rate of entrainer is represented as F_E.

3.2.2 Constraints

Desired product purities are respectively defined in Eqs. (2)–(4), which are executed as constraint function in Aspen Plus.

$$x_{EtOH} \geq x_{EtOH}^{desired} \tag{2}$$

$$x_{DMC} \geq x_{DMC}^{desired} \tag{3}$$

$$x_{PX} \geq x_{PX}^{desired} \tag{4}$$

where two product purities EtOH and DMC are both 99.90 mol% and the threshold recovery entrainer purity is 99.99 mol%.

3.2.3 Variable bounds

$$N_{F1}^{min} \leq N_{F1} \leq N_{F1}^{max} \tag{5a,b}$$

$$N_{FE}^{min} \leq N_{FE} \leq N_{FE}^{max} \tag{6a,b}$$

$$N_{F2}^{min} \leq N_{F2} \leq N_{F2}^{max} \tag{7a,b}$$

$$RR_1^{min} \leq RR_1 \leq RR_1^{max} \tag{8a,b}$$

$$RR_2^{min} \leq RR_2 \leq RR_2^{max} \tag{9a,b}$$

$$F_E^{min} \leq F_E \leq F_E^{max} \tag{10a,b}$$

$$D_1^{min} \leq D_1 \leq D_1^{max} \tag{11a,b}$$

$$D_2^{min} \leq D_2 \leq D_2^{max} \tag{12a,b}$$

The complete process optimization model involving objective function (Eq. (1)), constraints (Eqs. (2)–(4)) and variable bounds (Eqs. (5a,b)–(12a,b)) is defined as CPOM for the optimization

of the energy-saving EPSD scheme.

3.3 Process evaluation

3.3.1 Economic evaluation

TAC involving total operating and capital costs (i.e., TOC and TCC) as an economic indicator is reported by Douglas [44], which is illustrated as follow,

$$\mathrm{TAC} = \frac{\mathrm{TCC}}{\mathrm{PP}} + \mathrm{TOC} \tag{13}$$

where TOC contains steam and cooling water investments for heat exchangers (e.g., condenser, reboiler, and cooler). TCC involves equipment investments of heat exchangers and columns; PP denotes as payback period which is determined as three-year.

The shell and tray costs of the column are calculated as follow,

$$\text{shell cost [US\$]} = \frac{(\mathrm{M\&S})}{280} \times 101.9 \times D^{1.066} \times H^{0.802} \times (2.18 + F_{\mathrm{C}}) = 2252.28 \times D^{1.066} \times H^{0.802} \tag{14}$$

$$\text{tray cost [US\$]} = \frac{(\mathrm{M\&S})}{280} \times 4.7 \times D^{1.55} \times H \times F_{\mathrm{C}} = 1423.7 \times D^{1.55} \times H \tag{15}$$

where Marshall and Swift index (M&S) is assumed as 1518.1 [45]; H [m] and D [m] represent the height and the diameter; correction factor of the shell and tray (F_{C}) are determined as 1.9 and 55.9, respectively [45].

Capital costs for the reboiler, condenser, and heat exchanger are obtained as follow,

$$\text{heat exchanger cost [US\$]} = \frac{(\mathrm{M\&S})}{280} \times 101.3 \times A^{0.65} \times (2.29 + F_{\mathrm{C}}) = 9367.8 A^{0.65} \tag{16}$$

where A (m^2) denotes the area of reboiler, condenser, and heat exchanger; coefficients of the heat exchanger is 14.77 [45].

Calculations of area and heat transfer temperature difference for the reboiler and heat exchanger are displayed as follow,

$$A_{\mathrm{R}}\ [\mathrm{m}^2] = \frac{Q_{\mathrm{R}}}{(\Delta T_{\mathrm{R}} \times U_{\mathrm{R}})} \tag{17}$$

$$\Delta T_{\mathrm{R}}\ [^{\circ}\mathrm{C}] = T_{\mathrm{Steam}} - T_{\mathrm{R}} \tag{18}$$

$$\Delta T_{\mathrm{R}}\ [^{\circ}\mathrm{C}] = \frac{(T_{\mathrm{hin}} - T_{\mathrm{cout}}) - (T_{\mathrm{hout}} - T_{\mathrm{cin}})}{\ln(\frac{T_{\mathrm{hin}} - T_{\mathrm{cout}}}{T_{\mathrm{hout}} - T_{\mathrm{cin}}})} \tag{19}$$

where A_{R} [m^2] in Eq. (17) represents the area of the reboiler and heat exchanger; Q_{R} in MW is the reboiler duty; U_{R} = 568 W/m^2/°C is the heat transfer coefficient of the reboiler; T_{R} [°C] are the reboiler temperature; ΔT_{R} [°C] in Eq. (18) denotes the heat transfer temperature difference of reboiler; T_{Steam} represents the temperature of steam; ΔT_{R} [°C] in Eq. (19) denotes the heat transfer temperature difference of heat exchanger; the inlet and outlet temperatures of the high-temperature stream denote as T_{hin} and T_{hout}; the inlet and outlet temperature of the low-temperature stream represent T_{cin} and T_{cout}.

The calculations of area and heat transfer temperature difference for the condenser are shown as follow,

$$A_{\mathrm{C}}\ [\mathrm{m}^2] = \frac{Q_{\mathrm{C}}}{(\Delta T_{\mathrm{C}} \times U_{\mathrm{C}})} \tag{20}$$

$$\Delta T_{\mathrm{C}}\ [^{\circ}\mathrm{C}] = \frac{(T_{\mathrm{hin}} - T_{\mathrm{cout}}) - (T_{\mathrm{hout}} - T_{\mathrm{cin}})}{\ln(\frac{T_{\mathrm{hin}} - T_{\mathrm{cout}}}{T_{\mathrm{hout}} - T_{\mathrm{cin}}})} \tag{21}$$

where A_{C} [m^2] in Eq. (20) is the area of the condenser; Q_{C} [kW] is the condenser duty; U_{C} = 852 W/m^2/°C is the heat transfer coefficient of the condenser; ΔT_{C} is the logarithmic mean temperature difference, which is calculated via the Eq. (21); T_{cin} and T_{cout} are 30 and 40 °C while the cooling water is adopted [45].

Energy cost of the cooling water and steam could be calculated via the Eqs. (22) and (23).

$$\text{operating cost of cooling water [US\$/y]} = C_{\mathrm{CW}} \times Q_{\mathrm{C}} \times 8000 \tag{22}$$

$$\text{operating cost of steam [US\$/y]} = C_{\mathrm{Steam}} \times Q_{\mathrm{R}} \times 8000 \tag{23}$$

where C_{CW} = 0.354 US$/GJ is the cost of cooling water; C_{Steam} = 7.78, 8.22, and 9.88 US$/GJ denotes the cost of low-pressure (LP), medium-pressure (MP), and high-pressure (HP) steams.

3.3.2 Environmental assessment

Environment and sustainability impact of the existing and proposed processes could be evaluated by introducing indirect CO_2 emissions [46]. Of note is that, the computational of CO_2 emissions is a complex issue because of the steam could be produced via the natural gas, coal, and heavy oil [47, 48]. Hence, a simplified model for computing CO_2 emissions for the distillation system is proposed by Gadalla et al. [49], which is illustrated as follow,

$$(CO_2)_{emissions} = (\frac{Q_{fuel}}{NHV}) \times (\frac{C\%}{100})\alpha \quad (24)$$

where α denotes the molar mass ratio of CO_2-to-C, which is 3.67; the net heating value (abbreviated as NHV) is 39771 kJ/kg, and the carbon content C% is 86.5 kg/kg. Besides, the energy consumption of the fuel (Q_{fuel}, kJ) can be obtained as follows,

$$Q_{fuel} = \frac{Q_{seq}}{\lambda_{seq}} \times (h_{seq} - 419) \times (\frac{T_F - T_0}{T_F - T_S}) \quad (25)$$

where latent heat and enthalpy of the hot utility are expressed as λ_{seq} (kJ/kg) and h_{seq} (kJ/kg); Q_{seq} (kJ) represents the energy consumption of the process. Moreover, the reference temperature, T_0, is determined as 298.15K, flame temperature, T_F, is 2073.15K, stack temperature, T_S, is 433.15K.

3.3.3 Thermodynamic efficiency evaluation

Following the study of our previous studies [31, 50], exergy loss (El) could be used as another significant indicator to compare energy efficiency of the existing and proposed process. For a given system, the El in Eq. (26) could be obtained via the difference of input and output of exergy (Ex).

$$El = \sum Ex_{input} - \sum Ex_{output} \quad (26)$$

For a given specified system, Ex is computed via the enthalpy (H) and entropy (S) in Eq. (27).

$$Ex = (H - H_0) - T_0 \cdot (S - S_0) \quad (27)$$

where the $(H-H_0)$ and $(S-S_0)$ represent the enthalpy and entropy difference between the specified and the reference systems and the environment temperature (25 ℃) is denoted as T_0.

4. Computational Results and Discussion

4.1 Effect of pressure on the univolatility lines

Following the experimental study of Liu et al. [41], the UNIQUAC model is determined to describe the vapor-liquid equilibrium of ternary system EtOH/DMC/PX. The implemented (i.e., EtOH/DMC and EtOH/PX) and regressed (i.e., DMC/PX) binary interaction parameters in the Aspen Plus are summarized in Table 1.

Table 1. Interaction parameters of the UNIQUAC model for EtOH/DMC system with PX as entrainer.

Component i	DMC	EtOH	DMC
Component j	EtOH	PX	PX
Temperature units	℃	℃	℃
Data sources	NISTV84 NIST-RK	APV84 VLE-IG	[a]regression
Aij	-1.4291	4.0754	0.8583
Aji	-0.4662	-5.6391	-4.7936
Bij	871.3750	-1202.4300	-235.5900
Bji	183.7840	2504.2000	1822.8300
Cij	0.1000	0.3000	0.3000

[a]The regression parameters of DMC and PX can be referred to Li et al. [41].

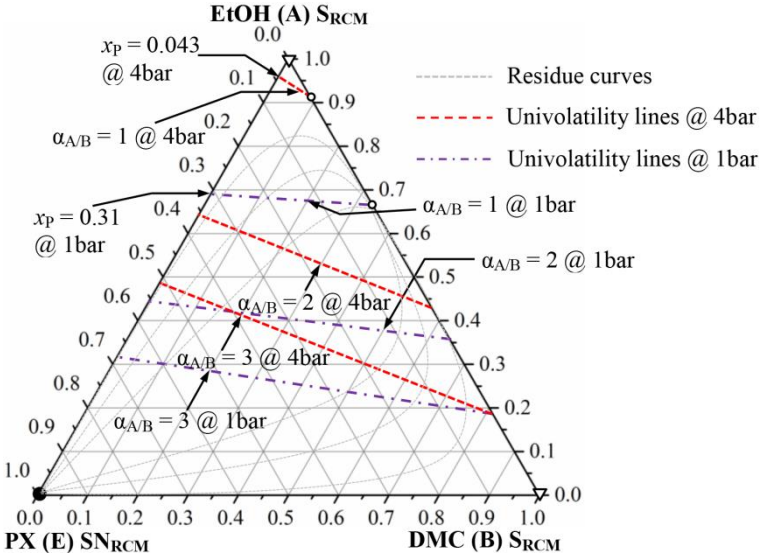

Figure 4. Effects of operating pressure on univolatility lines for DMC/EtOH/PX system

Effects of operating pressure on univolatility lines for the EtOH/DMC/PX system are demonstrated in Figure 4. Univolatility curves could be obtained via the Flash2 module in the Aspen Plus [31]. In this section, 4 bar is chosen as an initial value of the operating pressure and the optimal pressure will be determined in the next section. The value of x_P is located at 0.31 at the edge EtOH-PX under the pressure of 1.0 bar while the value of x_P equals 0.043 at 4.0 bar. Moreover, the intersections of $\alpha_{A/B}$ = 2 or 3 at the binary side EtOH-PX under 4.0 bar are lower than those under 1.0 bar. In summary, the minimum amount of entrainer could be effectively reduced at higher operating pressures.

4.2 Process optimization

Optimal EPSD scheme is obtained via the proposed optimization approach CPOM which is carried out on the desktop with Intel Core i5-7400 CPU@3.00GHZ, 8 GB memory. When the operating pressure of EDC is determined as 4.0 bar, the calculation of the whole optimization process takes about 1.5 h.

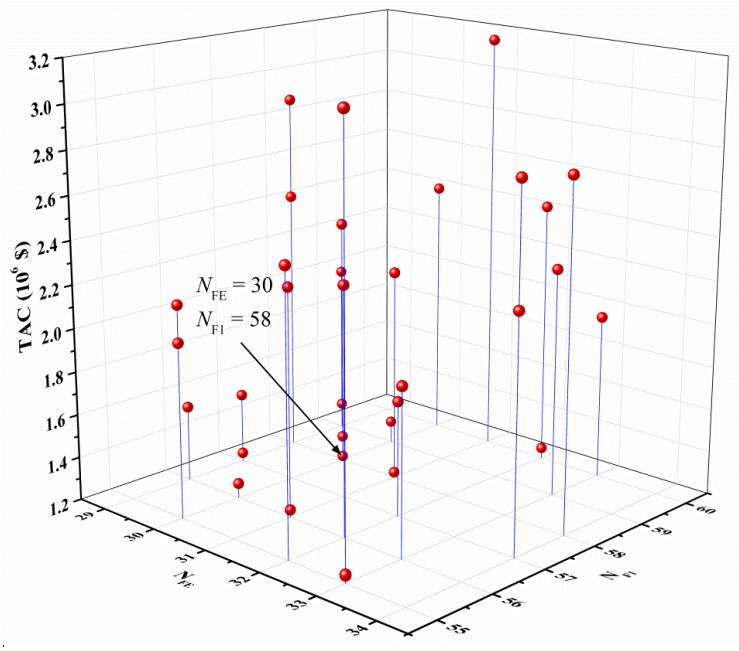

Figure 5. Effects of feed location of entrainer and fresh feed (N_{FE} and N_{F1}) on TAC

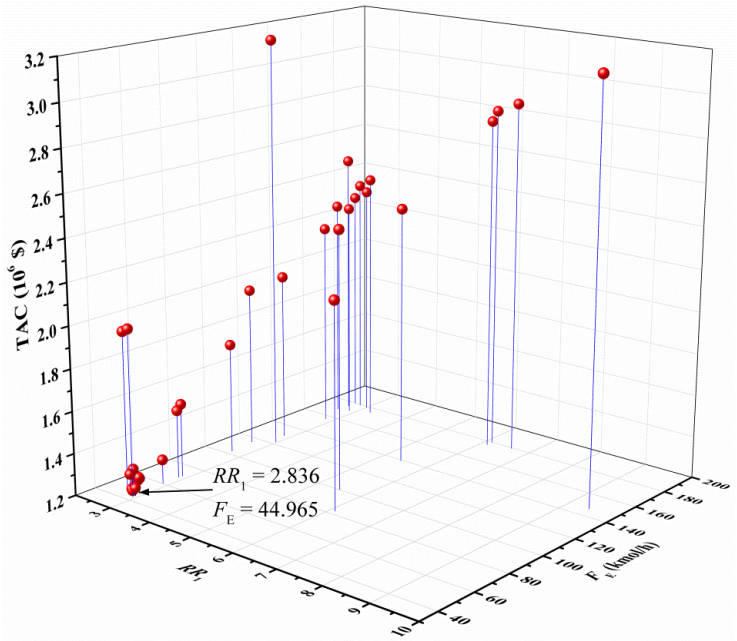

Figure 6. Effects of reflux ratio and flow rate of entrainer (RR_1 and F_E) on TAC

Continuous variables (e.g., distillate rates and reflux ratio) and discrete variables (e.g., feed locations and total number of stages) of the EDC are optimized with TAC as objective function. Effects of discrete variables feed location of entrainer and fresh feed (N_{FE} and N_{F1}) on TAC are demonstrated in Figure 5. The minimum TAC is obtained when the N_{FE} = 30 and N_{F1} = 58 are chosen. Figure 6 displays the effects of reflux ratio and flow rate of entrainer (RR_1 and F_E) on

TAC. The minimum TAC is obtained with $RR_1 = 2.836$ and $F_E = 44.965$ kmol/h.

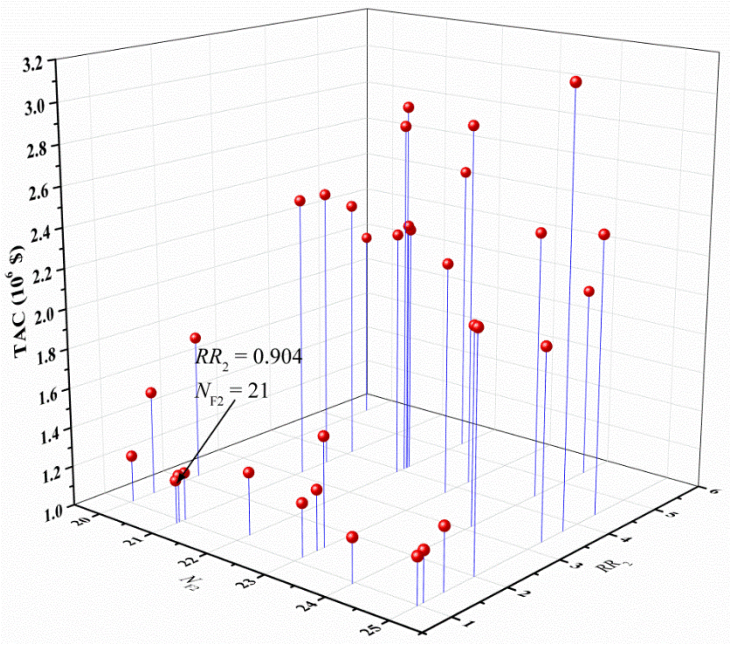

Figure 7. Effect of reflux ratio and feed location of ERC (RR_2 and N_{F2}) on TAC

Figure 7 illustrates the effect of reflux ratio and feed location of ERC (RR_2 and N_{F2}) on TAC. TAC is decreasing when reducing reflux ratio. $RR_1 = 0.904$ and $N_{F2} = 21$ are determined while the minimum TAC is obtained. In addition, the effect of distillate rates for EDC and ERC (D_1 and D_2) on TAC is displayed in Figure 8. $D_1 = 50.023$ and $D_2 = 50.039$ are determined to obtain 99.9 mol% DMC and EtOH with the minimum TAC.

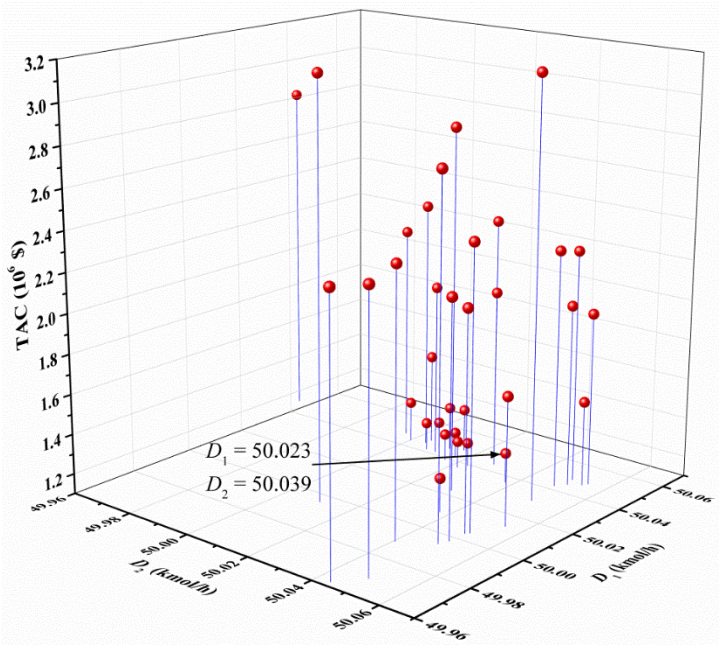

Figure 8. Effect of distillate rates of EDC and ERC (D_1 and D_2) on TAC

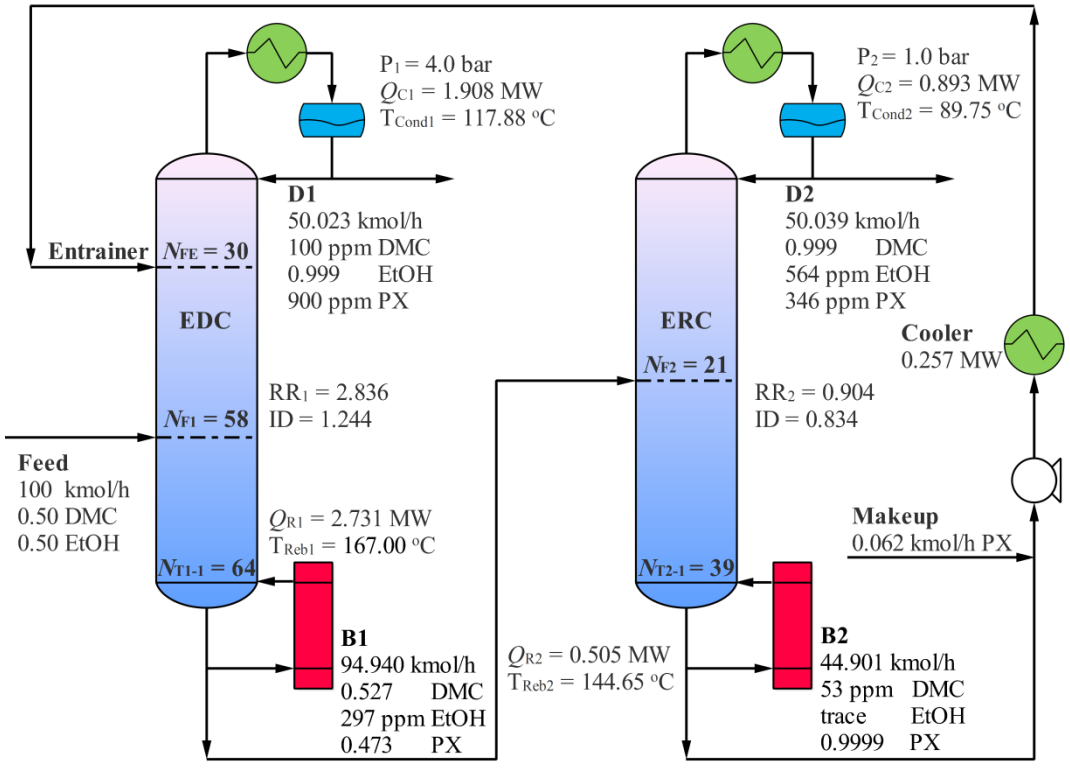

Figure 9. Optimal design of extractive pressure-swing distillation process for separating EtOH/DMC mixtures with P_1 = 4.0 bar

The optimal EPSD scheme with P_1 = 4.0 bar and P_2 = 1.0 bar (called as design 2) for the separation of binary azeotropic system DMC/EtOH with PX as entrainer is presented in Figure 9. The optimal fresh feed and entrainer are fed to 30th and 58th stages of the EDC, respectively. The

production EtOH of 99.90 mol% is obtained at the overhead of the EDC while the mole reflux ratio is 2.836. The bottom stream is then fed into 21th stage of the column ERC and the DMC of 99.90 mol% is distilled. Finally, reboiler duties of two columns are 2.731 and 0.505 MW, respectively.

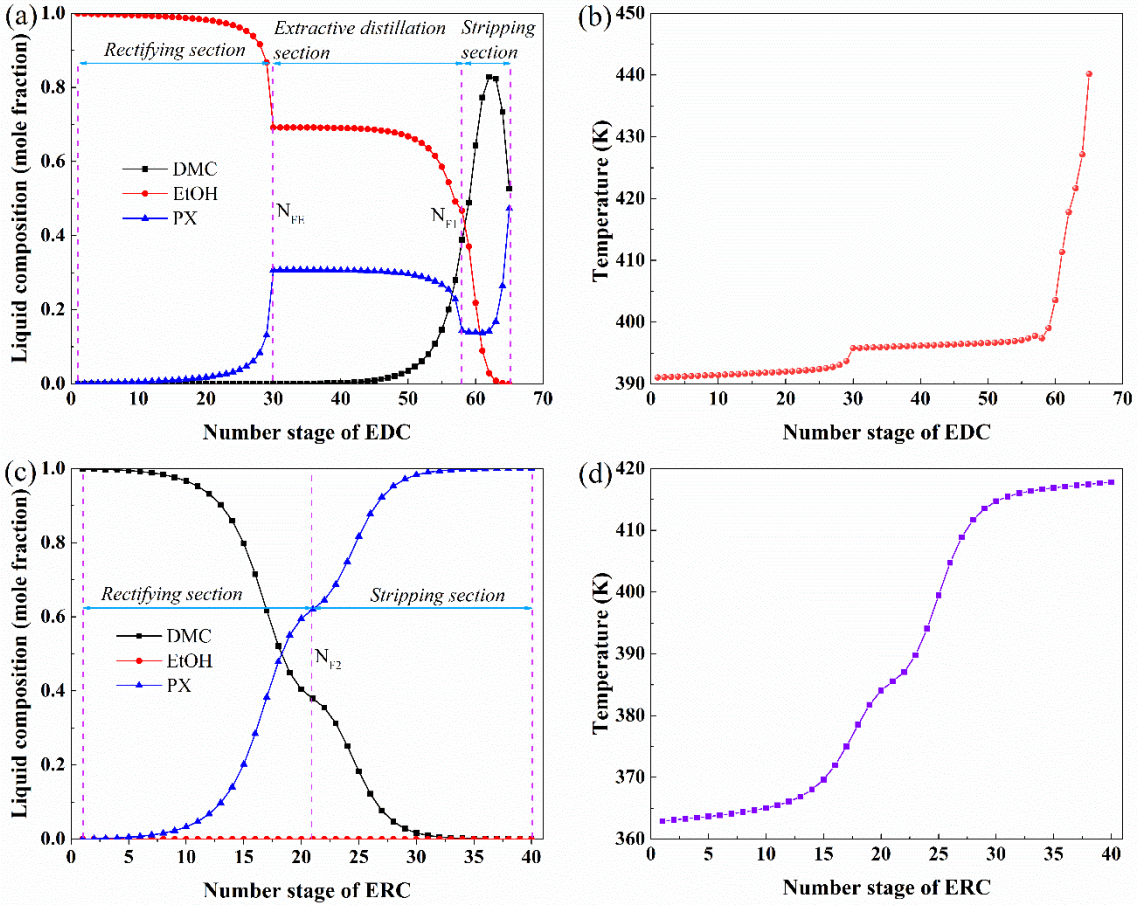

Figure 10. Composition and temperature profiles of (a,b) EDC and (c,d) ERC

To observe the reliability of the optimization results, composition and temperature profiles of the EDC and ERC in design 2 are represented in Figure 10. From Figure 10a, the composition of EtOH (marked as red circle) increases drastically between stages 58 and 30 because the extraction process is taken place in this extractive distillation section to broken the DMC/EtOH azeotrope. Following that, the EtOH is obtained as the distillate in the rectifying section (i.e., from 2th to 30th stages). At stage 1 (i.e., condenser), the EtOH composition achieves its highest

purity of 99.9 mol%. DMC and PX are obtained at the bottom of the stripping section and then are separated in the column ERC. In the rectifying section of ERC, DMC is distilled while the PX is obtained in the stripping section of ERC (see Figure 10c). Similar observations can be made for the temperature profiles of the EDC and ERC from Figure 10b,d.

From Figure 9, the reboiler duty of the proposed EPSD scheme is significantly reduced while the operating pressure of the EDC is increased. As such, the operating pressure of EDC should be optimized to further reduce the amount of entrainer and energy consumption. Of note is that, the operating pressure of distillation column has better not exceeding 10 bar [10, 35]. Effects of operating pressure (from 1 to 10 bar) on TAC and the flow rate of entrainer-to-feed flow rate (FE/F) are illustrated in Figure 11.

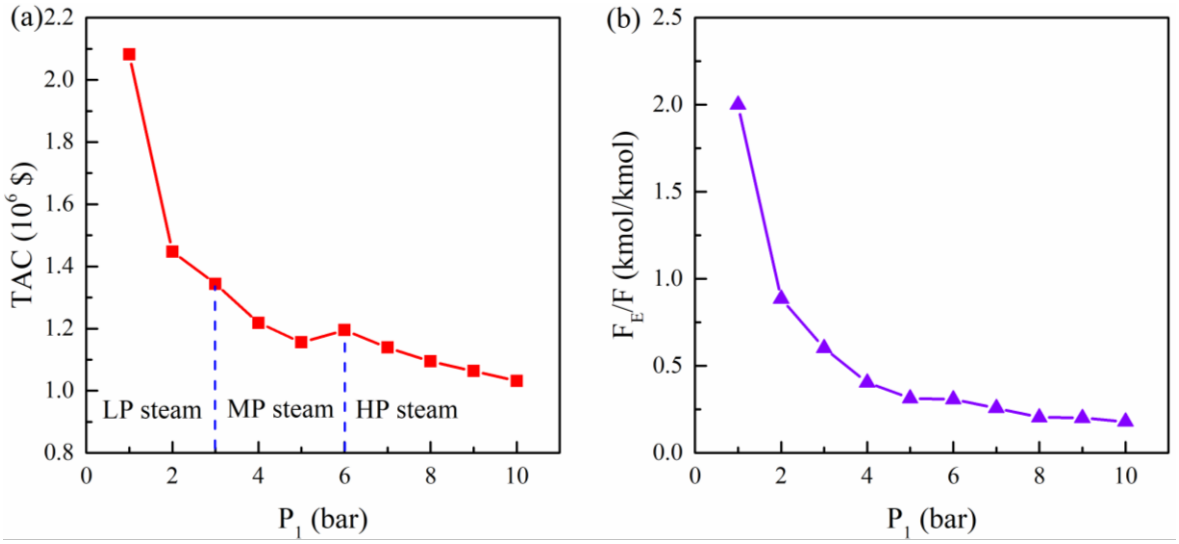

Figure 11. Effect of pressure on TAC and flow rate of entrainer-to-feed flow rate (F_E/F)

It can be observed from Figure 11a that the LP, MP and HP steams are used when the operating pressure are the [1,3), [3,6), and [6,10] bar, respectively. It is worth noting that the TAC at 6 bar is higher than that that at 5 bar because the more expensive HP steam is used. Moreover, F_E/F could be also reduced while increasing the pressure (see Figure 11b). Finally, P_1 = 10.0 bar is determined for the optimal EPSD with minimum TAC.

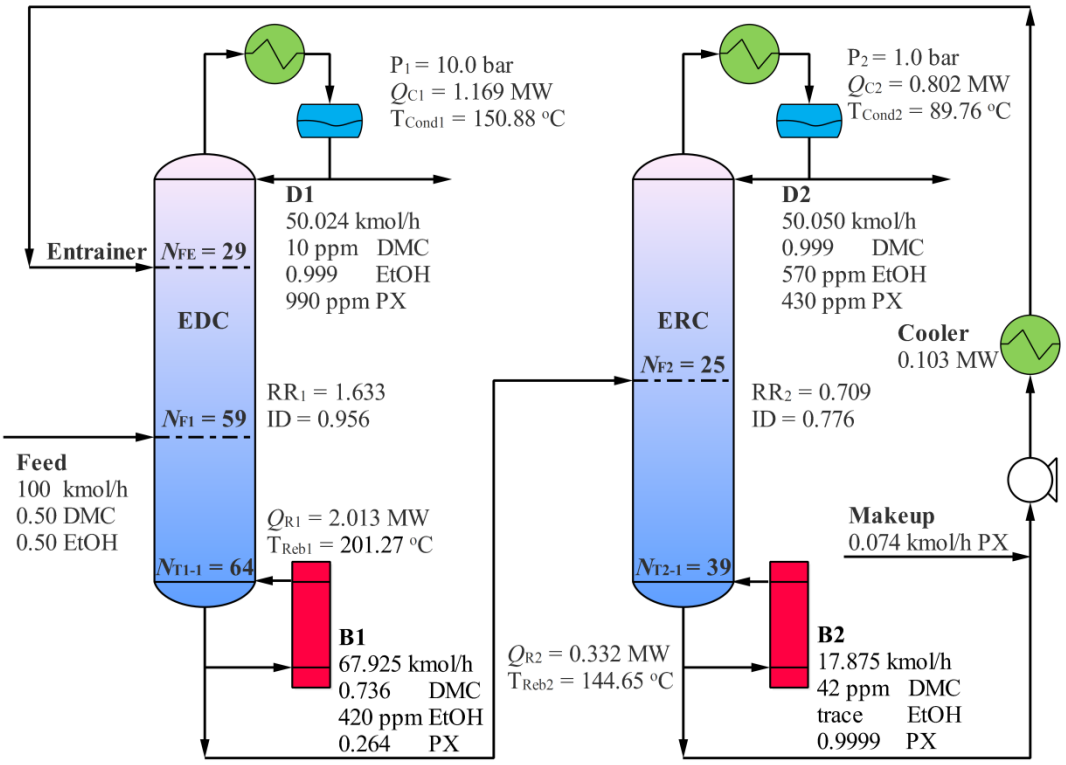

Figure 12. Optimal design of extractive pressure-swing distillation process for separating DMC/EtOH mixtures with P_1 = 10.0 bar (design 3)

Figure 12 displays the optimal EPSD scheme with P_1 = 10.0 bar and P_2 = 1.0 bar (called as design 3) for the separation of binary azeotropic system EtOH/DMC with PX as entrainer. Total numbers of stages of two columns are 65 and 40, respectively. For EDC, the optimal fresh feed and entrainer are fed to 29th and 59th stages, respectively. To obtain the production EtOH of 99.90 mol% at the overhead of the EDC, the mole reflux ratio of 1.633 is required. The bottom stream is then fed to 25th stage of the column ERC and the mole reflux ratio of 0.709 is determined. DMC of 99.90 mol% is distilled and PX of 99.99 mol% is obtained at the bottom stream. Finally, reboiler duties of two columns are 2.013 and 0.332 MW, respectively.

4.3 Heat integration

Heat integration for the EPSD scheme should be considered to further reduce the energy consumption because the extractive column is operated at a high pressure. From Figure 12, the temperature of the condenser in the EDC is 150.88 °C when P_1 is at 10 bar. Of note is that, there

is no enough temperature difference when P_2 is 1 bar because the temperature of the reboiler in the ERC is 144.65 °C. To achieve the heat integration, P_2 should be reduced. Effect of pressure on TAC for heat integration process is demonstrated in Figure 13.

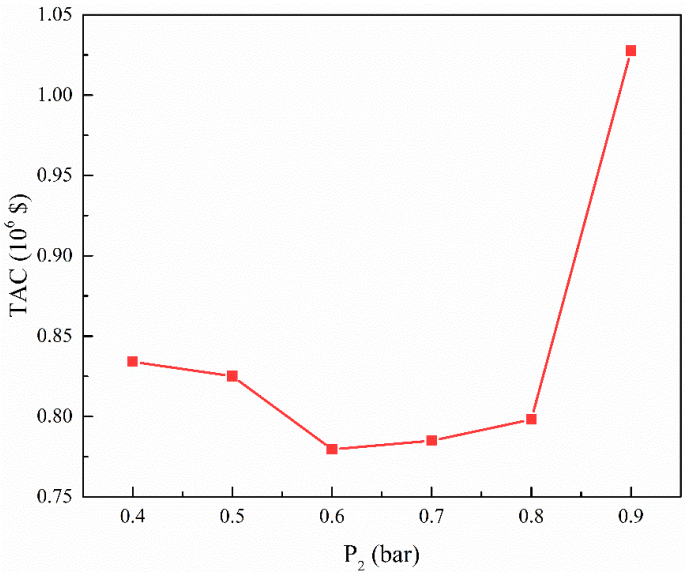

Figure 13. Effect of pressure on TAC for heat integration process

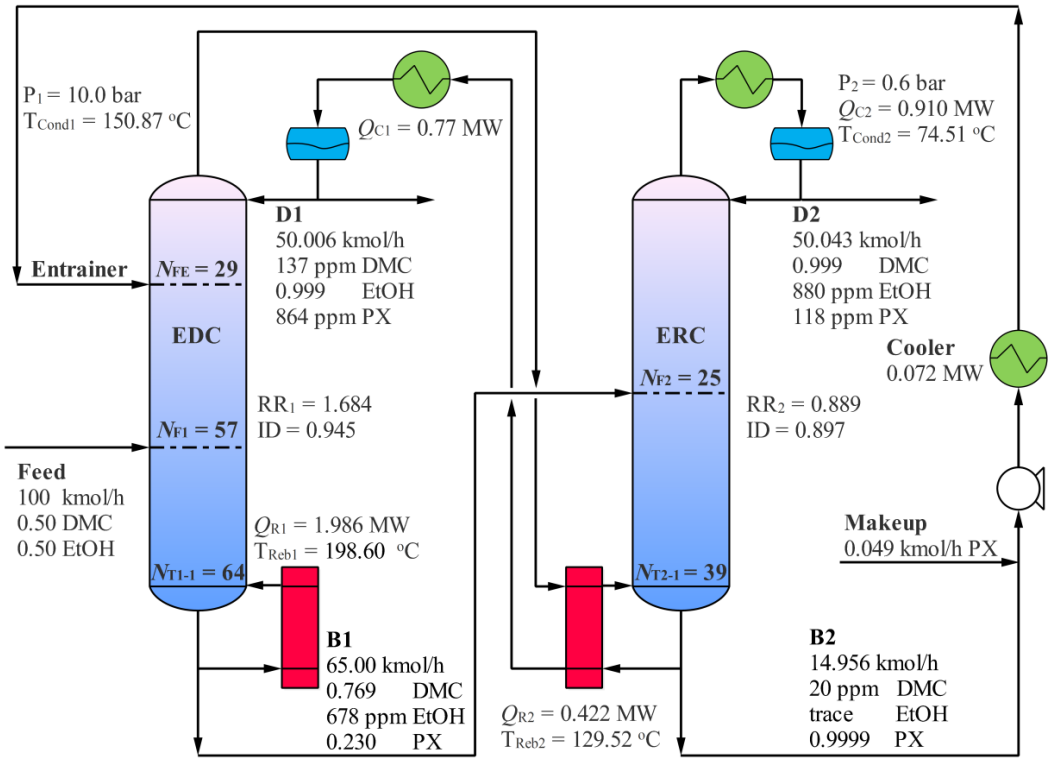

Figure 14. Optimal design of heat integration process for separating DMC/EtOH with P_1 = 10.0 bar and P_2 = 0.6 bar (design 4)

From Figure 13, the pressure of the ERC, P_2, at 0.6 bar achieves the lowest TAC for the heat

integration EPSD process. Figure 14 gives the optimal heat integration EPSD scheme (denoted as design 4) for the separation of binary azeotropic system EtOH/DMC with PX as entrainer. The 0.422 MW of reboiler duty in the ERC is provided via the vapor of condenser in the EDC. In addition, an auxiliary condenser is required with 0.77 MW for the EDC.

4.4 Economic and Environmental Evaluation

Table 2. Design parameters of the extractive distillation process for separating DMC/EtOH system with PX as entrainer.

	design 1	design 2	design 3	design 4
N_{T1}	65	65	65	65
N_{FE}	27	30	29	29
N_{F1}	51	58	59	57
P_1 (bar)	1.0	4.0	10.0	10.0
Q_{R1} (MW)	4.083	2.731	2.013	1.986
Q_{C1} (MW)	2.766	1.908	1.169	0.770
RR_1	4.076	2.836	1.633	1.684
F_E (kmol/h)	200.020	44.901	17.875	14.956
N_{T2}	40	40	40	40
N_{F2}	23	21	25	25
P_2 (bar)	1.0	1.0	1.0	0.6
Q_{R2} (MW)	1.712	0.505	0.332	-
Q_{C2} (MW)	1.811	0.893	0.802	0.910
RR_2	2.862	0.904	0.709	0.889
TOC ($\times 10^6$ US$/y)	**1.339**	**0.788**	**0.667**	**0.582**
TCC ($\times 10^6$ US$)	**2.230**	**1.127**	**0.866**	**0.590**
TAC ($\times 10^6$ US$/y)	**2.082**	**1.164**	**0.956**	**0.779**

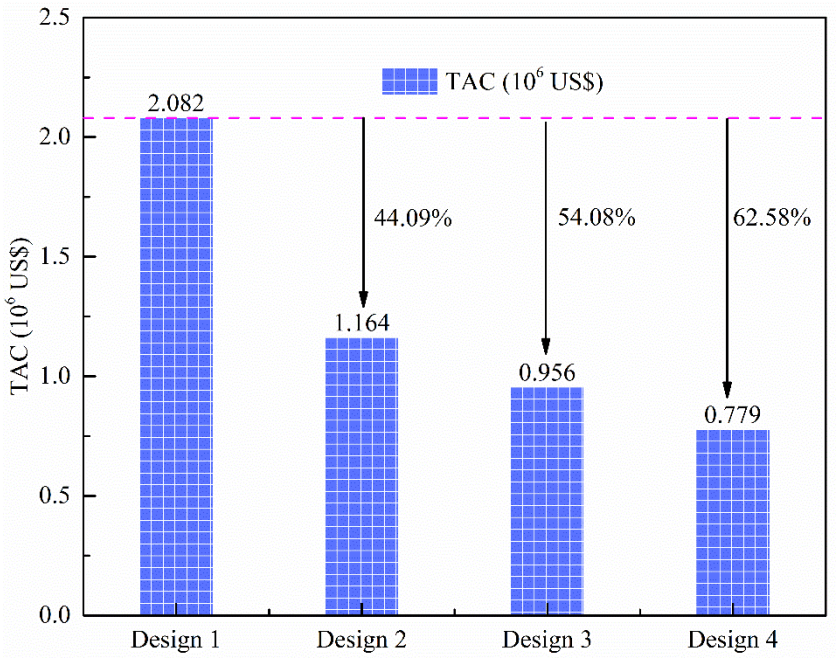

Figure 15. Economic comparisons of four design processes

The detailed economic comparisons between the four separation schemes are demonstrated in Figure 15 and Table 2. It can be observed that three proposed schemes (i.e., designs 2-4) have overwhelming advantages in economic benefits compared with that of the existing process (design 1). Hereby, compared with the existing process, the TAC of proposed designs 2-4 are reduced by 44.09%, 54.08%, and 62.58%, respectively. The computational result illustrates that the design 4 is the most promising configuration among the four DMC/EtOH separation processes attribute to the higher thermodynamic efficiency in reducing the energy requirements of the reboiler by 65.73%.

Table 3. Comparison of CO_2 emissions between existing and proposed processes.

	design 1	design 2	design 3	design 4
Q_{R1} (MW)	4.083	2.731	2.013	1.986
Q_{R2} (MW)	1.712	0.505	0.332	-
CO_2 emissions (kg/h)	**1959.019**	**1093.940**	**792.735**	**671.374**

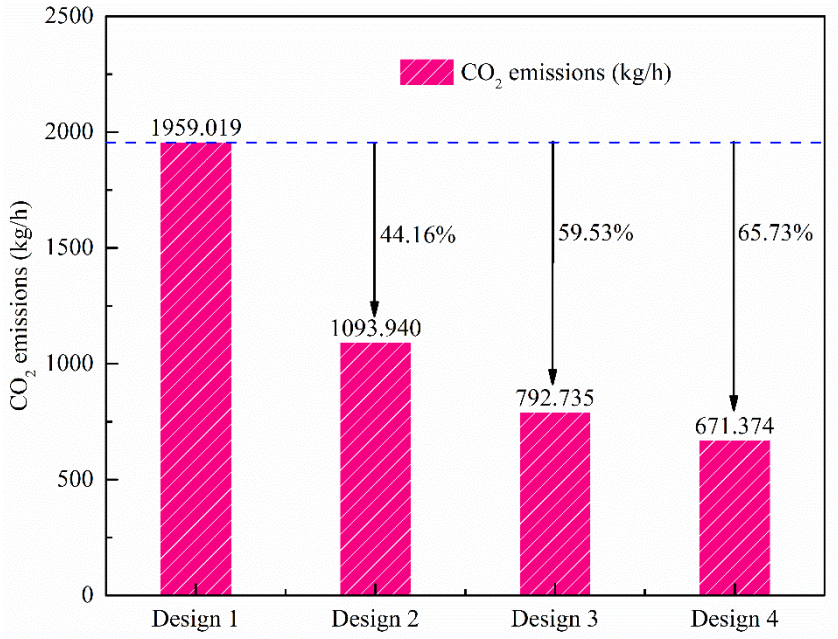

Figure 16. Environmental comparisons between four processes

A comparison of CO_2 emissions among the processes of three proposed designs and the existing design is listed in Table 3 and Figure 16. Compared with the existing process design 1, the CO_2 emissions of proposed schemes design 2-4 for separating DMC/EtOH are reduced by 44.16%, 59.53, and 65.73, respectively. These significant reductions mainly attribute to the reduction in total reboiler duties of the alternative separation schemes.

Table 4. Comparison of exergy loss between existing and proposed processes.

	design 1	design 2	design 3	design 4
EDC (kW)	417.532	223.583	155.133	144.899
Condenser 1 (kW)	318.245	384.697	305.024	200.829
Reboiler 1 (kW)	235.061	95.334	140.560	144.339
ERC (kW)	97.193	23.607	21.801	40.174
Condenser 2 (kW)	258.514	127.489	114.495	97.362
Reboiler 2 (kW)	43.917	12.924	8.501	15.947
Cooler (kW)	188.025	43.425	17.434	10.898
Total exergy loss (kW)	**1558.487**	**911.059**	**762.948**	**654.448**

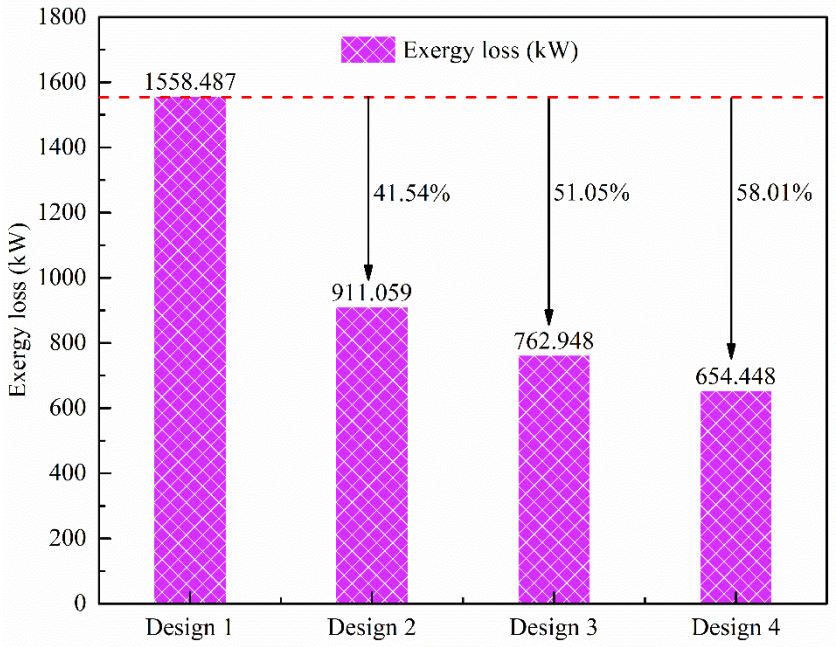

Figure 17. Thermodynamic comparisons between four design processes

The calculations of exergy loss for the three proposed designs and the existing design are displayed in Table 4 and Figure 17. Evidently, exergy loss of three proposed schemes (designs 2-4) could be reduced by 41.54%, 51.05%, and 58.01% compared with that of the existing process design 1, which is mainly attributed to the reduction of heat duty.

In summary, the proposed sustainable extractive pressure-swing distillation process show promising not only on TAC but also significantly reduces the exergy loss. Additionally, it displays benefits in carbon dioxide emissions.

5. Conclusion

A novel extractive pressure-swing distillation (EPSD) scheme for separating minimum azeotropic mixtures ethanol and dimethyl carbonate is proposed to achieve the performance of energy-saving, reduction of carbon dioxide emissions and enhancing of thermodynamic efficiency. Effects of the pressure on univolatility lines are investigated to reduce the minimum flow rate of entrainer. Following that, the design parameters (e.g., feed locations and reflux ratio)

and pressure are optimized based on the minimum total annual cost. The results showed that the proposed EPSD with P_1 = 4.0 bar and P_2 = 1.0 bar (design 2) can save 44.09% of total annual cost (TAC) compared with that of the existing scheme (i.e., $P_1 = P_2$ = 1.0 bar). Meanwhile, the CO_2 emissions and exergy loss of the design 2 could be reduced by 44.16% and 41.54%, respectively. Following that, TAC, CO_2 emissions, and exergy loss could be further decreased when the operating pressure of extractive distillation column is determined as 10 bar (design 3). TAC of the proposed design 4 with heat integration (i.e., P_1 = 1.0 bar and P_2 = 0.6 bar) can save 62.58%. CO_2 emissions of the proposed design 4 can reduce 65.73% compared with the design 1. Moreover, it is found that the exergy loss of the design 4 is reduced by 58.01% compared with the design 1 (i.e., $P_1 = P_2$ = 1.0 bar).

Of note is that the proposed approach could be widely extended to separate other similar systems (e.g., acetonitrile/benzene/methanol) to recover valuable resources and pursue sustainable development. Moreover, the control structure of the proposed heat-integrated process will be further explored in another work because of the highly-coupled issues.

Acknowledgments

We acknowledge the financial support provided by the National Natural Science Foundation of China (Nos. 21878028, 21606026); the Fundamental Research Funds for the Central Universities (Nos. 2019CDQYHG021, 2019CDXYHG0012).

References:

[1] J. Ma, W. Li, C. Ni, Y. Li, S. Huang, C. Shen, C. Xu, Investigation of distillation systems using heavy or intermediate entrainers for separating toluene-methanol: process economics and control, Journal of Chemical Technology & Biotechnology, 91 (2016) 2111-2124.

[2] J.A. Jaime, G. Rodríguez, I.D. Gil, Control of an optimal extractive distillation process with mixed-solvents as separating agent, Industrial & Engineering Chemistry Research, 57 (2018) 9615-9626.

[3] Q. Zhang, M. Liu, C. Li, A. Zeng, Design and control of extractive distillation process for separation of the minimum-boiling azeotrope ethyl-acetate and ethanol, Chemical Engineering Research and Design, 136 (2018) 57-70.

[4] Y. Hu, Y. Su, S. Jin, I.L. Chien, W. Shen, Systematic approach for screening organic and ionic liquid solvents in homogeneous extractive distillation exemplified by the tert-butanol dehydration, Separation and Purification Technology, 211 (2019) 723-737.

[5] A. Yang, T. Shi, S. Sun, S. Wei, W. Shen, J. Ren, Dynamic controllability investigation of an energy-saving double side-stream ternary extractive distillation process, Separation and Purification Technology, 225 (2019) 41-53.

[6] X. Gao, B. Zhu, J. Ma, D. Yang, A combination of pressure-swing and extractive distillation for separating complex binary azeotropic system, Chemical Engineering and Processing: Process Intensification, 122 (2017) 269-276.

[7] S. Sun, L. Lü, A. Yang, S. Wei, W. Shen, Extractive distillation: Advances in conceptual design, solvent selection, and separation strategies, Chinese Journal of Chemical Engineering, (2018). DOI: 10.1016/j.cjche.2018.08.018

[8] Q. Zhang, M. Liu, C. Li, A. Zeng, Heat-integrated pressure-swing distillation process for separating the minimum-boiling azeotrope ethyl-acetate and ethanol, Separation and Purification Technology, 189 (2017) 310-334.

[9] Y. Ma, Y. Luo, S. Zhang, X. Yuan, Simultaneous optimization of complex distillation systems

and heat integration using pseudo-transient continuation models, Computers & Chemical Engineering, 108 (2018) 337-348.

[10] A. Yang, W. Shen, S. Wei, L. Dong, J. Li, V. Gerbaud, Design and control of pressure-swing distillation for separating ternary systems with three binary minimum azeotropes, AIChE Journal, 65 (2019) 1281-1293.

[11] C. Wang, Z. Zhang, X. Zhang, C. Guang, J. Gao, Comparison of pressure-swing distillation with or without crossing curved-boundary for separating a multiazeotropic ternary mixture, Separation and Purification Technology, 220 (2019) 114-125.

[12] S. Liang, Y. Cao, X. Liu, X. Li, Y. Zhao, Y. Wang, Y. Wang, Insight into pressure-swing distillation from azeotropic phenomenon to dynamic control, Chemical Engineering Research and Design, 117 (2017) 318-335.

[13] K. Mishra, N. Kaistha, Synthesis, design, and control of an azeotropic distillation system for methanol–isopropyl acetate separation, Industrial & Engineering Chemistry Research, 58 (2018) 1229-1243.

[14] Y. Dai, F. Zheng, B. Xia, P. Cui, Y. Wang, J. Gao, Application of mixed solvent to achieve an energy-saving hybrid process including liquid–liquid extraction and heterogeneous azeotropic distillation, Industrial & Engineering Chemistry Research, 58 (2019) 2379-2388.

[15] Z. Han, Y. Ren, H. Li, X. Li, X. Gao, Simultaneous extractive and azeotropic distillation separation process for production of PODEn from formaldehyde and methylal, Industrial & Engineering Chemistry Research, 58 (2019) 5252−5260.

[16] J. Pla-Franco, E. Lladosa, S. Loras, J.B. Montón, Azeotropic distillation for 1-propanol dehydration with diisopropyl ether as entrainer: equilibrium data and process simulation,

Separation and Purification Technology, 212 (2019) 692-698.

[17] A. Yang, S. Jin, W. Shen, P. Cui, I.L. Chien, J. Ren, Investigation of energy-saving azeotropic dividing wall column to achieve cleaner production via heat exchanger network and heat pump technique, Journal of Cleaner Production, 234 (2019) 410-422.

[18] X. Li, S. Wang, Y. Wang, P. Cui, D. Xu, Z. Zhu, Optimization of decanter temperature in separating partially miscible homoazeotrope to reduce cost and energy consumption, Journal of Chemical Technology & Biotechnology, 94 (2019) 1998-2008.

[19] D.S. Sholl, R.P. Lively, Seven chemical separations to change the world, Nature, 532 (2016) 435-437.

[20] A.A. Kiss, D.J.P.C. Suszwalak, Enhanced bioethanol dehydration by extractive and azeotropic distillation in dividing-wall columns, Separation and Purification Technology, 86 (2012) 70-78.

[21] A. Yang, R. Wei, S. Sun, S. Wei, W. Shen, I.L. Chien, Energy-saving optimal design and effective control of heat integration-extractive dividing wall column for separating heterogeneous mixture methanol/toluene/water with multiazeotropes, Industrial & Engineering Chemistry Research, 57 (2018) 8036-8056.

[22] S. Tututi-Avila, N. Medina-Herrera, J. Hahn, A. Jiménez-Gutiérrez, Design of an energy-efficient side-stream extractive distillation system, Computers & Chemical Engineering, 102 (2017) 17-25.

[23] L. Sun, Q. Wang, L. Li, J. Zhai, Y. Liu, Design and control of extractive dividing wall column for separating benzene/cyclohexane mixtures, Industrial & Engineering Chemistry Research, 53 (2014) 8120-8131.

[24] C. Wang, C. Guang, Y. Cui, C. Wang, Z. Zhang, Compared novel thermally coupled extractive distillation sequences for separating multi-azeotropic mixture of acetonitrile/benzene/methanol, Chemical Engineering Research and Design, 136 (2018) 513-528.

[25] Y.-C. Chen, S.-K. Hung, H.-Y. Lee, I.L. Chien, Energy-saving designs for separation of a close-boiling 1,2-propanediol and ethylene glycol mixture, Industrial & Engineering Chemistry Research, 54 (2015) 3828-3843.

[26] W. Shen, L. Dong, S. Wei, J. Li, H. Benyounes, X. You, V. Gerbaud, Systematic design of an extractive distillation for maximum-boiling azeotropes with heavy entrainers, AIChE Journal, 61 (2015) 3898-3910.

[27] Y.-H. Wang, I.L. Chien, Unique Design Considerations for maximum-boiling azeotropic systems via extractive distillation: acetone/chloroform separation, Industrial & Engineering Chemistry Research, 57 (2018) 12884-12894.

[28] Y. Zhao, T. Zhao, H. Jia, X. Li, Z. Zhu, Y. Wang, Optimization of the composition of mixed entrainer for economic extractive distillation process in view of the separation of tetrahydrofuran/ethanol/water ternary azeotrope, Journal of Chemical Technology & Biotechnology, 92 (2017) 2433-2444.

[29] T. Shi, A. Yang, S. Jin, W. Shen, S. Wei, J. Ren, Comparative optimal design and control of two alternative approaches for separating heterogeneous mixtures isopropyl alcohol-isopropyl acetate-water with four azeotropes, Separation and Purification Technology, 225 (2019) 1-17.

[30] Q. Pan, X. Shang, J. Li, S. Ma, L. Li, L. Sun, Energy-efficient separation process and control scheme for extractive distillation of ethanol-water using deep eutectic solvent, Separation and Purification Technology, 219 (2019) 113-126.

[31] A. Yang, H. Zou, I.L. Chien, D. Wang, S. Wei, J. Ren, W. Shen, Optimal design and effective control of triple-column extractive distillation for separating ethyl acetate/ethanol/water with multiazeotrope, Industrial & Engineering Chemistry Research, 58 (2019) 7265−7283.

[32] C. Cui, J. Sun, Rigorous design and simultaneous optimization of extractive distillation systems considering the effect of column pressures, Chemical Engineering and Processing - Process Intensification, 139 (2019) 68-77.

[33] L. Li, L. Guo, Y. Tu, N. Yu, L. Sun, Y. Tian, Q. Li, Comparison of different extractive distillation processes for 2-methoxyethanol/toluene separation: design and control, Computers & Chemical Engineering, 99 (2017) 117-134.

[34] X. You, I. Rodriguez-Donis, V. Gerbaud, Low pressure design for reducing energy cost of extractive distillation for separating diisopropyl ether and isopropyl alcohol, Chemical Engineering Research and Design, 109 (2016) 540-552.

[35] X. You, J. Gu, C. Peng, W. Shen, H. Liu, Improved design and optimization for separating azeotropes with heavy component as distillate through energy-saving extractive distillation by varying pressure, Industrial & Engineering Chemistry Research, 56 (2017) 9156-9166.

[36] J. Gu, X. You, C. Tao, J. Li, W. Shen, J. Li, Improved design and optimization for separating tetrahydrofuran–water azeotrope through extractive distillation with and without heat integration by varying pressure, Chemical Engineering Research and Design, 133 (2018) 303-313.

[37] J. Gu, X. You, C. Tao, J. Li, V. Gerbaud, Energy-saving reduced-pressure extractive distillation with heat integration for separating the biazeotropic ternary mixture tetrahydrofuran–methanol–water, Industrial & Engineering Chemistry Research, 57 (2018) 13498-13510.

[38] X. Zhang, X. Li, G. Li, Z. Zhu, Y. Wang, D. Xu, Determination of an optimum entrainer for

extractive distillation based on an isovolatility curve at different pressures, Separation and Purification Technology, 201 (2018) 79-95.

[39] S. Jin, A.J. Hunt, J.H. Clark, C.R. McElroy, Acid-catalysed carboxymethylation, methylation and dehydration of alcohols and phenols with dimethyl carbonate under mild conditions, Green Chemistry, 18 (2016) 5839-5844.

[40] A. Yang, S. Sun, A. Eslamimanesh, S. Wei, W. Shen, Energy-saving investigation for diethyl carbonate synthesis through the reactive dividing wall column combining the vapor recompression heat pump or different pressure thermally coupled technique, Energy, 172 (2019) 320-332.

[41] K. Liu, Z. Wang, Y. Zhang, D. Xu, J. Gao, Z. Ma, Y. Wang, Vapour-liquid equilibrium measurements and extractive distillation process design for separation of azeotropic mixture (dimethyl carbonate + ethanol), The Journal of Chemical Thermodynamics, 133 (2019) 10-18.

[42] W. Shen, V. Gerbaud, Extension of thermodynamic insights on batch extractive distillation to continuous operation. 2. azeotropic mixtures with a light entrainer, Industrial & Engineering Chemistry Research, 52 (2013) 4623-4637.

[43] W. Shen, H. Benyounes, V. Gerbaud, Extension of thermodynamic insights on batch extractive distillation to continuous operation. 1. azeotropic mixtures with a heavy entrainer, Industrial & Engineering Chemistry Research, 52 (2013) 4606-4622.

[44] J.M. Douglas, Conceptual design of chemical processes, McGraw-Hill New York, 1988.

[45] W.L. Luyben, Distillation design and control using Aspen simulation, John Wiley & Sons, 2013.

[46] Y. Zhao, K. Ma, W. Bai, D. Du, Z. Zhu, Y. Wang, J. Gao, Energy-saving thermally coupled

ternary extractive distillation process by combining with mixed entrainer for separating ternary mixture containing bioethanol, Energy, 148 (2018) 296-308.

[47] X. You, I. Rodriguez-Donis, V. Gerbaud, Reducing process cost and CO_2 emissions for extractive distillation by double-effect heat integration and mechanical heat pump, Applied Energy, 166 (2016) 128-140.

[48] Ž. Olujić, L. Sun, A. de Rijke, P.J. Jansens, Conceptual design of an internally heat integrated propylene-propane splitter, Energy, 31 (2006) 3083-3096.

[49] M. Gadalla, Z. Olujic, A. Derijke, P. Jansens, Reducing CO_2 emissions of internally heat-integrated distillation columns for separation of close boiling mixtures, Energy, 31 (2006) 2409-2417.

[50] A. Yang, L. Lv, W. Shen, L. Dong, J. Li, X. Xiao, Optimal design and effective control of the tert-amyl methyl ether production process using an integrated reactive dividing wall and pressure swing columns, Industrial & Engineering Chemistry Research, 56 (2017) 14565-14581.